ELSEVIER

An illumination distribution preserved colour substitution algorithm based on dichromatic reflection model

Z.G. Pan[a], P. Wang[a,b], J.H. Xin[b,*], M.M. Zhang[a], H.L. Shen[b]

[a]*State Key Lab of CAD&CG, Zhejiang University, Hangzhou 310027, China*
[b]*Institute of Textiles and Clothing, The Hong Kong Polytechnic University, Hong Kong, China*

Abstract

In this paper, we introduce a novel colour substitution algorithm based on the dichromatic reflection model. We separate the object colour and scene illumination information in the target area of the original image. The object colour was subsequently substituted while keeping the illumination information unchanged. A new method was employed to estimate the object colour. We also developed a set of new parameters to adjust the intensity distribution on the resultant image. Our algorithm is totally automatic and can achieve more realistic effects compared with other colour substitution methods.
© 2005 Elsevier B.V. All rights reserved.

1. Introduction

Colour substitution is widely used in many fields such as image synthesis, virtual reality and image based rendering. It is especially useful in virtual exhibition, internet purchasing and computer-aided design applications. In recent years, some related works have been presented in the literature [9,12,20]. For example, Reinhard et al. [12] presented a method to render the colour appearance of a colour image using that of another image based on a decorrelated colour space. Inspired by that work, Ashikhmin et al. [18] proposed an algorithm to colourize a grayscale image by selecting target swatches from other colour images. Most recently, Levin et al. [9] presented a simple but quite interesting method to colourize grayscale images and video clips, according to the assumption that neighbouring pixels with similar intensities should also have similar colours. These methods seem to perform well for images of natural scenes. However, these works are all based on the statistical distribution of colour channels, and often require intensive user-interaction. Most importantly, they do not

consider the physical interaction between light source and object surface. As a consequence, they may not be suitable for the colourization of three-dimensional objects, especially in the case of highlight. Therefore, it is still worthwhile and challenging to develop a robust and real-time algorithm for the colour substitution of natural and human-made objects.

Considering an object in different scenes, the changes of its colour appearances are not only in the luminance channel but also in the chromatic channels. We use the dichromatic reflection model proposed by Shafer and Klinker [4,13] to separate the illuminant effects and the real colour of an object. The dichromatic model describes the surface reflection behaviour of inhomogeneous dielectrics, for example, paints, plastics, cloth, paper and some natural objects. Under the dichromatic reflection model, the light reflected from the object surface is divided into two different parts of reflections physically, interface or surface part and body or subsurface part.

The dichromatic reflection model has been proved to be correct experimentally by many researchers [8,15]. Recently, this model was widely used for surface reflection parameters estimation [15,17], illuminant calculation [1,2,7,14] and images processing [3,5,16,19]. Traditional dichromatic reflection model algorithms project the input signals onto a colour signal plane using orthogonal

---

* Corresponding author. Tel.: +852 2766 6474; fax: +852 2773 1432.
E-mail address: tcxinjh@inet.polyu.edu.hk (J.H. Xin).

decomposition methods such as SVD. Then the dots on the plane are fitted with a kind of prescient shape, as described in [17], to compute the two base vectors, the body colour and the illuminant colour. However, these algorithms seem to work well only on the images coming from highly saturated objects under well-controlled imaging conditions. The interface reflection is generally not very saturated as it has the similar colour with the illuminant. Therefore for unsaturated objects, the interface and body colour signals are close. In this case, the estimation of colour signal plane may be unreliable.

In our algorithm, a new project method is developed to estimate the body and interface colour vectors directly. To deal with the lowly saturated body colour, we introduced an intensity contrast adjustment to achieve realistic result. Compared with some colour substitution methods which use intensity directly, for example [11], our method considers the effects of the colour constancy carefully. Compared with other colour substitution algorithms or proprietary applications [6,10,20], an advantage of our algorithm is the total automaticity. Only the source image and new body colour are demanded from users. It helps to avoid the distortions caused by inaccuracy of additional inputs such as illuminant colour and referenced colour. We have applied our algorithm to a computer-aided clothes design system and obtained satisfactory results.

To make the result more realistic, a texture mapping technique is employed when users want to substitute with a texture image other than a single colour. A texture grid is interactively built to map the texture. In [11], a similar method is mentioned. However, the grid design course in our method is more convenient.

In Section 2, the background of our technique is introduced. The implementation is described in Section 3. In Section 4, we compare our technique with others. In Section 5, a conclusion is made.

2. Background

2.1. Colour signal formation

The response of the spectral distribution of reflected light can be described as

$$\rho = \int_w P(\lambda)V(\lambda)d\lambda \tag{1}$$

where λ is the wavelength parameter, $P(\lambda)$ is the spectral power distribution, and $V(\lambda)$ is the sensitivity function of the imaging device or human eyes. Integration is performed over the visible spectrum w. The spectral power distribution $P(\lambda)$ depends on both the surface-reflectance $S(\lambda)$ and the spectral power distribution of the illuminant $E(\lambda)$.

2.2. Dichromatic reflection model

The dichromatic reflection model is a mathematical structure of surface-reflectance functions on inhomogeneous substances, which are composed of different component materials including a vehicle at the surface layer and embedded pigments at the colourant layer. Typical examples of inhomogeneous substances are plastics and paints. When light reaches the inhomogeneous surface, one part is reflected at the interface between the surface and the air, the other part enters the surface and is scattered by the pigment particles. This part of light can only be observed after it crosses the surface again into the air. Therefore, the reflected light $P(\lambda)$ is described as

$$P(\theta, \lambda) = P_I(\theta, \lambda) + P_S(\theta, \lambda) \tag{2}$$

where θ represents the reflection geometry, including the incident angle, the viewing angle, and the phase angle. The subscripts I and S denote the interface and subsurface reflection, respectively.

The dichromatic reflection model assumes that the spectral composition of each reflected light component is independent of the geometric conditions, which means that the geometry factors and the spectral factors can be separated. Since the reflected illumination is the product of the incident light and the surface-reflectance, Eq. (2) can be written as follows

$$P(\theta, \lambda) = C_I(\theta)S_I(\lambda)E(\lambda) + C_S(\theta)S_S(\lambda)E(\lambda) \tag{3}$$

where $S_I(\lambda)$ and $S_S(\lambda)$ are the spectral surface-reflectance functions for these two components. $E(\lambda)$ is the spectral power distribution of the incident light. $C_I(\theta)$ and $C_S(\theta)$ are the geometric factors.

Another assumption of the dichromatic reflection model is that the spectral composition of the interface reflection component is approximately the same as that of the incident light, except for an intensity change [13], which means that the reflectance of the interface component is constant over the visible wavelength, i.e. $S_I(\lambda) = \text{constant}$.

3. Algorithm implementation

3.1. Normalized illumination colour estimation

As described in the dichromatic reflection model, every colour signal in the object area is the linear combination of two colour vectors, $C_p = \alpha_p C_b + \beta_p C_i$, where C_b, C_i are body colour and illumination colour, respectively. α_p, β_p represents the geometric factors.

When we get an image, some operations should be adopted to remove the effects of the colour temperature. A pure white patch will be imaged in the same scene. Then the initial image is normalized with respect to the average colour of the white patch image. Therefore, the sensor
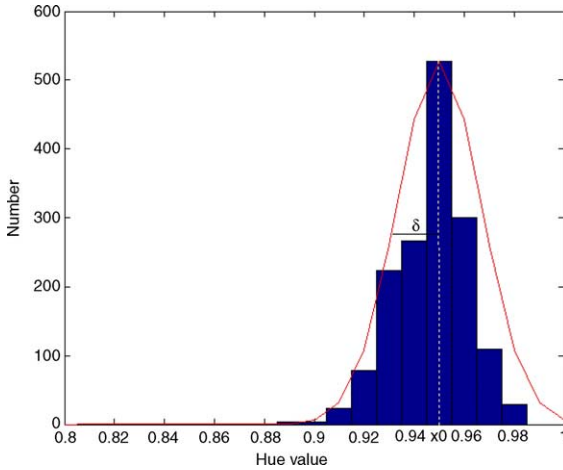
Fig. 1. Hue histogram used to get sample signals.

outputs of R, G and B channels are balanced to satisfy Eq. (4)

$$\int_w E(\lambda)V_R(\lambda)\mathrm{d}\lambda = \int_w E(\lambda)V_G(\lambda)\mathrm{d}\lambda = \int_w E(\lambda)V_B(\lambda)\mathrm{d}\lambda \qquad (4)$$

For most images recorded by digital camera, the camera will adjust the device sensitivity functions to achieve this effect.

As the dichromatic reflection model assumes that the interface reflectance is constant over the visible wavelength, we can find that the interface part of the reflected light has the same values in RGB channels after the white balance process. Therefore, we use the vector {1,1,1} to identify the illumination colour C_i.

3.2. Normalized body colour estimation

To avoid the distortion caused by noises, we should re-sample these original colour signals first. According to the definition of HSV colour space and the white illumination colour estimated in Section 3.1, colour signals from the same object should have the same hue values ideally. Therefore, the hue channel is adopted as the sample criterion. The hue histogram is calculated and fitted to a Gaussian function, as Fig. 1 shows. x_0 is the medium value and δ is the deviation value. All the colour signals whose hue values are between $[x_0-\delta, x_0+\delta]$ are selected as the sample signals.

As dichromatic reflection model describes, all sample vectors are the linear combination of C_b and C_i. When they are normalized, the vector that has the largest separation angle with C_{in} is the estimated value of C_{bn}. We use a simple project to find such a vector. First, we normalize all sample vectors. Then we project them onto the plane Ψ, which is perpendicular to C_{in} and across the original point. All resultant dots are on a line section PQ on Ψ. The dot P corresponds to C_{bn}. Therefore, we can calculate the coordinates of P and project it back to find C_{bn}. The total projection procedure is shown in Fig. 2. The projection formulas are given as follows: $\forall p \in S_S$, $C_p = \{R_p\ G_p\ B_p\}$, $C_{pn} = \{R_{pn}\ G_{pn}\ B_{pn}\}$

$$\begin{cases} x_p = \dfrac{2 \times R_{pn} - G_{pn} - B_{pn}}{3} \\ y_p = \dfrac{2 \times G_{pn} - R_{pn} - B_{pn}}{3} \end{cases} \qquad (5)$$

where x_p, y_p are coordinates of P on Ψ, C_{pn} is the normalized vector of C_p that satisfies $R_{pn}^2 + G_{pn}^2 + B_{pn}^2 = 1$. Given a dot on Ψ, the re-projection can be accomplished by solving Eq. (5).

We can simply select the far vertex (according to the original point) as the projected dot of C_b. In practices, however, not all the samples are on Φ exactly. In other words, not all the projected dots on Ψ are on the same line exactly. The reason is due to the non-linearity of the camera output and the information loss caused by image compression or processing. Therefore, a vectorization process is employed. The average slope of these projected dots is used to decide the line which fits them best. Fig. 3 shows the vectorization process. As an example, P and N are changed to P' and N'.

3.3. Colour substitution

In this section, the normalized illumination and body colour vectors are calculated. We decompose all the input signals with these two vectors in a least square sense to calculate the parameter sets α_P and β_P.

In the traditional dichromatic reflection model algorithms, the maximum value in the set α_P, α_{max}, is thought to be the amplitude of C_b [17], because this value corresponding to such a place (in the well controlled scene) where the incident angle is very small and the including angle between the view and reflection directions is very large.

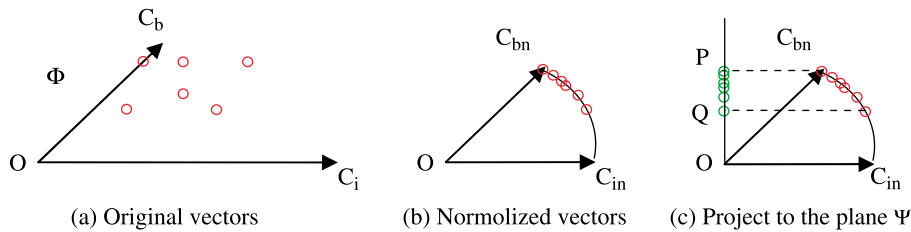(a) Original vectors   (b) Normolized vectors   (c) Project to the plane Ψ
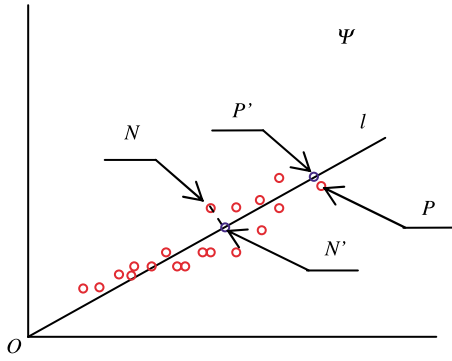
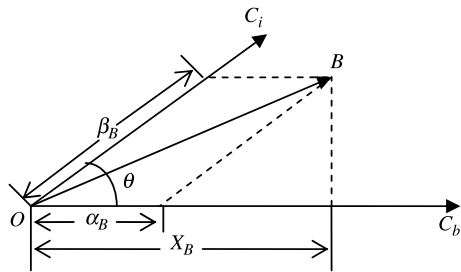Fig. 2. Projection procedure.

Fig. 3. Vectorization.

Fig. 4. Intensity on the body colour.

This means the subsurface component from this kind of place is dominating while the interface component is so small that can be ignored. Unfortunately, such a place does not necessarily exist in natural scenes. In most cases, we cannot estimate the amplitude of C_b accurately.

Instead of calculating the exact amplitude of the body colour, we select a special dot on the α–β plane and use the colour corresponding to it as the reference colour. The reference colour is the actual colour which will be substituted. We first select all the dots in which β values are near to zero. Then the maximum α value among them is the amplitude of the reference colour.

To keep the intensity contrast scope proportional to the new colour, a new parameter format should be developed. As Fig. 4 shows, the intensity of dot B on the body colour component is X_B. Then the new parameter form is given as

$$\begin{cases} \alpha' = \dfrac{\alpha + \beta \times \cos(\theta)}{n} \\ \beta' = \beta \end{cases} \tag{6}$$

where n is the amplitude of reference colour. For the colour substitution, the parameters α and β are calculated by solving Eq. (6) and n is replaced by the norm of the new colour.

In many situations, users want to paste a texture onto the target area. In this case, a texture mapping method should be employed to achieve realistic results. We developed a texture mapping technique base on a texture grid [21]. The texture grid is used to indicate the texture directions. The area covered by a patch of the grid has the texture directions indicated by the boundary of the patch. Our texture mapping technique can be divided into five steps as:

Step 1. Texture frame lines preprocessing.
Step 2. Virtual grid generation.
Step 3. Virtual grid combination.
Step 4. Texture grid adjustment.
Step 5. Texture coordinates calculation.

Details of these steps are discussed in [21]. For each pixel in the target image, a corresponding texture colour can be found using its texture coordinates. The colour substitution algorithm mentioned in the previous sections can be employed. The target image is analyzed first. For each pixel, the resultant colour can be calculated using its texture colour as the new colour. Because of the linearity of our algorithm, we only analyze the target image once during the colour combination course. Therefore, the colour combination step can be carried out rapidly.

(a) Original image

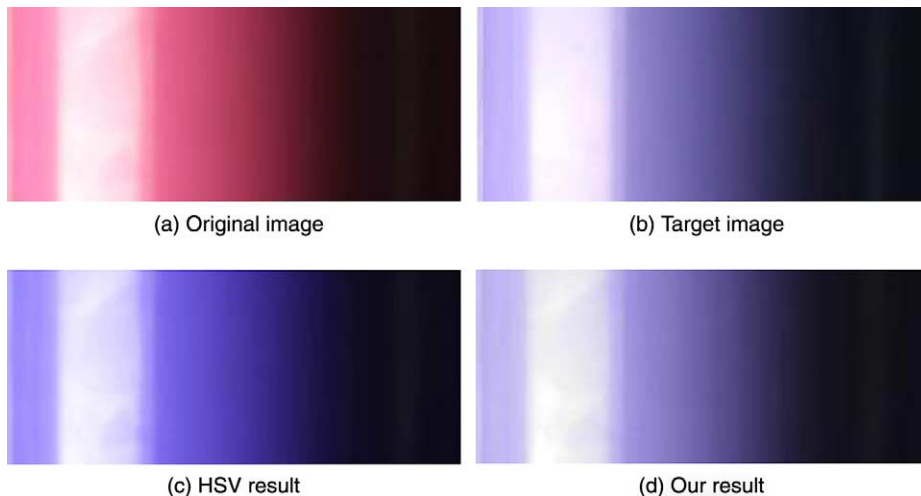(b) Target image

(c) HSV result

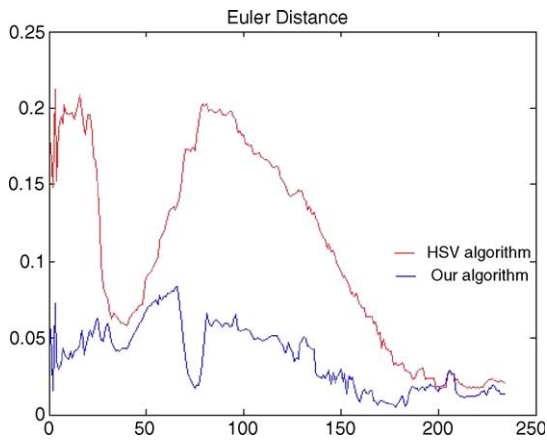(d) Our result

Fig. 5. Colour substitution experiment.

Fig. 6. Comparison of Euler differences calculated from our algorithm and HSV algorithm.

Table 1
Euler differences in different saturation ranges

Algorithms	Saturation range		
	[0, 0.1)	[0.1, 0.2]	(0.2, 1]
Our algorithm	0.0592	0.0602	0.0401
HSV algorithm	0.0813	0.1343	0.1533

4. Experimental results and comparisons

An experiment was designed to test the result of our algorithm. Two plastic cups, which are the same except for their colours, were placed at the same position in a fixed scene and images were taken using a digital camera Canon EOS D30. The images are processed using our algorithm to calculate the two reference colours. These colours are thought to be the corresponding new colours,

respectively. Then we use the parameter sets calculated from one image and the new colour of the other to construct a resultant image. We also select the algorithm based on the HSV colour spaces to compare with ours. In this algorithm, all colour values in the target image are transformed into HSV colour space. Then the hue values of all pixels are replaced by the hue value of new colour to build the resultant image. In Fig. 5, (a) is the original image, (b) is the target image, (c) is the HSV algorithm result and (d) is our result. It can be clearly found that our algorithm can give the closest colour information and intensity distribution to the real image. To make a quantitative comparison, we calculate the average colour value of each column of the (b)–(d) images in Fig. 5. Then for each column, the Euler differences: $\sqrt{\Delta R^2 + \Delta G^2 + \Delta B^2}$ between (c), (d) images and (b) image are calculated. The results are shown in Fig. 6. The difference of our algorithm is much smaller than the one of HSV algorithm. Another comparison is made according to different saturation ranges. We select all the columns whose intensity values are larger than 0.2. Then they are grouped according to their saturation values and the averages of these groups are calculated. Table 1 shows the results. For our algorithm, the average differences in all ranges are much smaller, because the two cups have a little difference in material quantity, that is more obvious in the unsaturated part of the images. The Euler differences of [0, 0.1), [0.1, 0.2] saturation ranges are larger than that of the last range. For HSV algorithm, the Euler difference of (0.2, 1] saturation range is even larger than that of the other ranges.

An example is shown in Fig. 7. It shows that our colour substitution algorithm can preserve the effects of
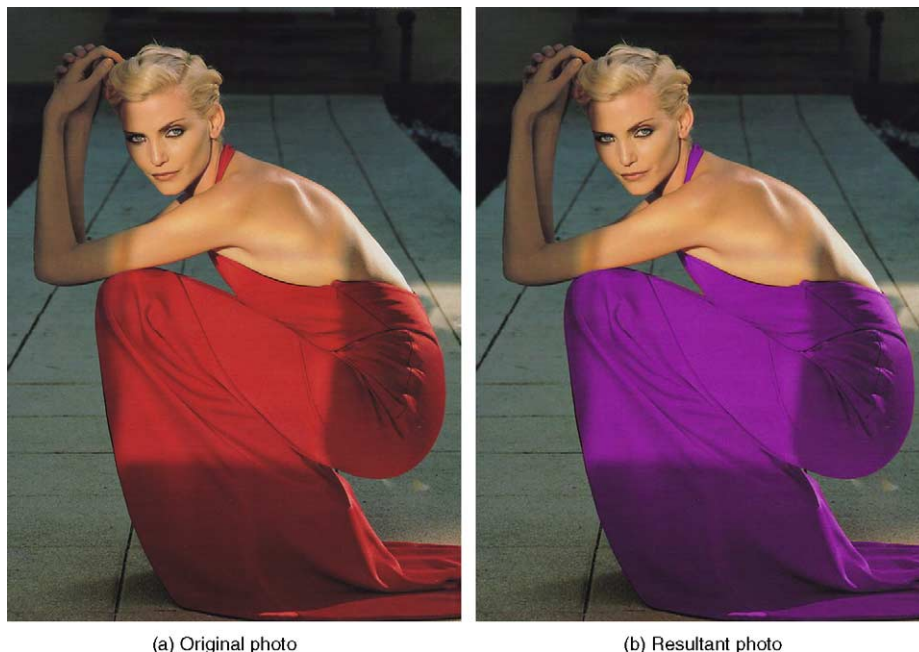

(a) Original photo   (b) Resultant photo

Fig. 7. Example 2.

(a) Original photo

(b) Texture 1

(c) Resultant photo

(d) Texture 2

Fig. 8. Example 3.

illumination very well and the resulting images' colour looks reasonable. Another example is given in Fig. 8. The twists on the wrinkles of the one-piece dress are reflected by the pattern of the texture image. The intensity distribution is maintained after the colour combination step.

5. Conclusion

We propose a novel colour substitution algorithm based on the dichromatic reflection model in this paper. A new project method is employed to estimate the body colour vector. We also develop a set of new parameters to adjust the intensity distribution to make the result natural and realistic. Through experiment, we find that our result is close to the real image when compared with other algorithms. Our algorithm is image based and totally automatic. Therefore, it is very suitable to the applications based on the internet. However, as described in [15], the constant interface reflectance assumption is not very suitable to some kinds of matters such as silk and metal. Therefore, to develop a colour substitution algorithm suitable for these kinds of matters is one of our future works.

Acknowledgements

References

[1] M. D'Zmura, P. Lennie, Mechanisms of colour constancy, J. Opt. Soc. Am. A 3 (10) (1986) 1662–1672.

[2] G.D. Finlayson, G. Schaefer, Convex and non-convex illuminant constraints for dichromatic colour constancy, Proc. IEEE Comput. Soc. Conf. Comput. Vis. Pattern Recogn. 1 (2001) 598–604.

[3] P. García, F. Pla, I. Gracia, Detecting edges in colour images using dichromatic differences, Proc. Seventh Int. Conf. Image Process. Appl. IEE 465 (1999) 363–367.

[4] G.J. Klinker, S. Shafer, T. Kanade, The measurement of highlights in colour images, Int. J. Comput. Vis. 2 (1) (1988) 7–32.

[5] V. Kravtchenko, J.J. Little, Efficient colour object segmentation using the dichromatic reflection model, Proc. IEEE Pacific Rim Conf. Commun. Comput. Signal Process. 1999; 90–94.

[6] Lectra, see http://www.lectra.com/en/index.php.

[7] H.C. Lee, Method for computing the scene-illuminant from specular highlights, J. Opt. Soc. Am. A 3 (10) (1986) 1694–1699.

[8] H.C. Lee, E.J. Breneman, C. Schulte, Modeling light reflection for computer colour vision, IEEE Trans. Pattern Anal. Mach. Intell. 12 (1990) 402–409.

[9] A. Levin, D. Lischinski, Y. Weiss, Colourization using optimization, Proc. ACM SIGGRAPH 2004; 689–694.

[10] L. Liu, G. Xu, Colour change method based on dichromatic reflection model, Proc. ICSP 1996; 1246–1249.

[11] J.L. Pellicer, J.S. Blanes, M.C. Sellés, 3D realistic—an image mapping system and its multimedia and internet integration, Proc. EUROGRAPHICS 2003; 27–34.

[12] E. Reinhard, M. Ashikhmin, B. Gooch, P. Shirley, Colour transfer between images, IEEE Comput. Graphics Appl. 21 (2001) 34–41.

[13] S. Shafer, Using colour to separate reflection components, Colour Res. Appl. 10 (1985) 210–218.

[14] S. Tominaga, A multi-channel vision system for estimating surface and illuminant functions, J. Opt. Soc. Am. A 13 (1996) 2163–2173.

[15] S. Tominaga, Dichromatic reflection models for rendering object surfaces, J. Imaging Sci. Technol. 40 (6) (1996) 549–555.

[16] S. Tominaga, Surface identification using the dichromatic reflection model, IEEE Trans. Pattern Anal. Mach. Intell. 13 (7) (1991) 658–670.

[17] S. Tominaga, N. Tanaka, Estimating reflection parameters from a single colour image, IEEE Comput. Graphics Appl. 20 (2000) 58–66.

[18] T. Welsh, M. Ashikhmin, K. Mueller, Transferring colour to grayscale images, ACM SIGGRAPH 2002; 277–280.

[19] S. Wesolkowski, S. Tominaga, R.D. Dony, Shading and highlight invariant colour image segmentation using the MPC algorithm, SPIE Colour Imaging: Device-Independent Colour, Colour Hardcopy, and Graphic Arts VI, 2001, pp. 229–240.

[20] P. Wang, M.M. Zhang, Z.G. Pan, A new texture morphing method for visual presentation of textile product, Proc. ICIG'2002, 2002; 1011–1016.

[21] P. Wang, M.M. Zhang, J.H. Xin, Z.G. Pan, H.L. Shen, An image-based texture mapping technique for apparel products exhibition and interior design, Displays 24 (4–5) (2003) 179–186.